

## 6. SIMPLIFICATION AND APPLICATION OF 'MODEL F'

The aim of Chapter 6 is to simplify and to demonstrate the possible applications of 'model F'. This chapter contains the following parts : firstly, the crack propagation rates calculated using 'model F' are related to those obtained using Paris equations (2.25) and (2.27), which leads to new crack propagation rate equation. Next the 'model F' is used to develop a *simplified* fatigue crack propagation model - 'model SF'. Finally, both 'model F' and 'model SF' are applied to two example problems.

### 6.1 'MODEL F' VERSUS PARIS EQUATION

Both 'model F' and the Paris equation can simulate fatigue crack propagation. Therefore, it should be possible to relate crack propagation rates calculated using 'model F' and the Paris equations. The *reason* for this is to simplify the procedures used to determine constants  $C$  and  $m$  of the Paris equations. A conventional experimental determination procedure is not always possible. Some attempts have already been made to determine the constants  $C$  and  $m$  using analytical rather than experimental methods ([6.1], [6.2]).

In addition to the constants  $C$  and  $m$ , the *modified* Paris equation (2.27) takes into account the fatigue threshold. Further, two aspects related to the Paris equation are evaluated on the basis of 'model F' : constants  $C$  and  $m$ , and fatigue threshold. Finally, a crack propagation rate equation similar to the Paris equation, is presented.

#### 6.1.1 Paris Equation Constants

In this section, analytical formulas for the constants used in the Paris equation are developed. This is done in following manner : a relationship between the effective stress intensity factor range  $\Delta K_{eff}$  and the crack propagation rate  $da/dN$  is established using the modeling principles of 'model F' (Chapter 3). Next, the constants  $C$  and  $m$  are extracted from established relationships.

An average crack propagation rate  $da/dN$  over the length  $\delta$  is a function of the fatigue life of the first element at the crack tip,  $N_{f,elem}$  :

$$\frac{da}{dN} = \frac{\delta}{N_{f,elem}} \quad (6.1)$$

$N_{f,elem}$  in Equation (6.1) can be determined by *iterating* the strain life relationship (3.11). However, an *analytical* formula for the  $N_{f,elem}$  is needed here. Assuming that the cyclic strains at the fatigue crack tip are dominantly *plastic*, the fatigue life of element  $N_{f,elem}$  can be determined using the *plastic* part (2.19) of the strain-life relationship. Equation (2.19) leads to the following formula for the  $N_{f,elem}$  :

$$N_{f,elem} = \frac{1}{2} \cdot \left( \frac{1}{2 \cdot \epsilon_f'} \cdot \Delta \epsilon_{pl} \right)^{\frac{1}{c'}} \quad (6.2)$$

Using the *plastic* part of the Ramberg-Osgood equation (3.20), it is possible to write the plastic strain range  $\Delta \epsilon_{pl}$  in Equation (6.2) as a function of plastic stress range :

$$\Delta \epsilon_{pl} = 2 \cdot \left( \frac{\Delta \sigma_{pl}}{2 \cdot K'} \right)^{\frac{1}{n'}} \quad (6.3)$$

Including only the *plastic* component of Glinka's ESED *range* criterion (3.30) permits the plastic stress range  $\Delta\sigma_{pl}$  in Equation (6.3) to be expressed as a function of linear-elastic stress range  $\Delta\sigma_{le}$  :

$$\Delta\sigma_{pl} = 2 \cdot K' \cdot \left[ \frac{n'+1}{\delta \cdot E \cdot K'} \right]^{\frac{n'}{n'+1}} \cdot (\Delta\sigma_{le})^{\frac{2-n'}{n'+1}} \quad (6.4)$$

The linear-elastic stress range  $\Delta\sigma_{le}$  in Equation (6.4) can be calculated using Equation (3.18). Taking  $j=1$  and substituting the  $\Delta\sigma_{le}$  and  $\Delta K_{eff}$  for the  $\sigma_{le,j}$  and  $K_{eff}$  in Equation (3.18) leads to :

$$\Delta\sigma_{le} = \Delta K_{eff} \cdot \sqrt{\frac{2}{\pi \cdot \delta}} \quad (6.5)$$

Making the substitutions as indicated in Figure 6.1 leads to the relationship between  $\Delta K_{eff}$  and  $da/dN$ , similar to the Paris equation :

$$\frac{da}{dN} = C_{pl} \cdot \Delta K_{eff}^{m_{pl}} \quad (6.6)$$

The constants  $C_{pl}$  and  $m_{pl}$  can be pre-calculated (Equations 6.7 and 6.8) and are functions of material parameters used in 'model F'. Equation (6.7) contains the element size  $\delta$ , but its influence on  $C_{pl}$  is not significant (see Chapter 5 about the influence of  $\delta$ ).

$$C_{pl} = 2 \cdot \delta \cdot \left( \varepsilon_f' \cdot \left( \frac{4 \cdot \pi \cdot \delta \cdot K' \cdot E}{n'+1} \right)^{\frac{1}{n'+1}} \right)^{\frac{1}{c'}} \quad (6.7)$$

$$m_{pl} = -\frac{2}{c' \cdot (n'+1)} \quad (6.8)$$

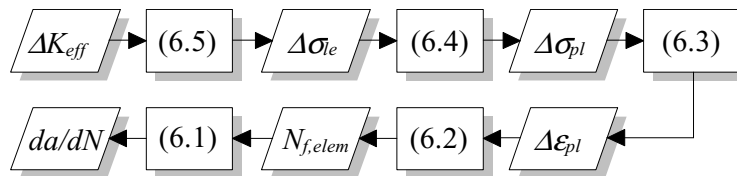


**Figure 6.1** : Substitutions made in order to obtain Equation (6.6).

## 6.1.2 Fatigue Threshold

In this section, formulas which take into account the *fatigue threshold* in relationship to  $da/dN$ - $\Delta K_{eff}$ , are developed using the modeling principles of 'model F'. It is assumed, that near the fatigue threshold where the  $\Delta K_{eff}$  is close to the  $\Delta K_{th}$ , the strain *ranges* at crack tip are *elastic* and not plastic. This implies that the fatigue life of the element at the crack tip,  $N_{f,elem}$  in Equation (6.9), can be calculated using the *elastic* part (2.18) of the strain-life relationship. Equation (2.18) leads to the following formula for the  $N_{f,elem}$  :

$$N_{f,elem} = \frac{1}{2} \cdot \left( \frac{E}{2 \cdot (\sigma_f' - \sigma_m)} \cdot \Delta\varepsilon_{el} \right)^{\frac{1}{b'}} \quad (6.9)$$

The elastic strain range  $\Delta\varepsilon_{el}$  in Equation (6.9) can be calculated using the linear-elastic stress range  $\Delta\sigma_{le}$  and the elastic modulus  $E$  (Equation 6.10). The  $\Delta\sigma_{le}$  in Equation (6.9) can be calculated using Equation (6.5).

$$\Delta\varepsilon_{el} = \frac{\Delta\sigma_{le}}{E} \quad (6.10)$$

Making the substitutions as indicated in Figure 6.2 leads to the following relationship between  $\Delta K_{eff}$  and  $da/dN$  :

$$\frac{da}{dN} = C_{el} \cdot \Delta K_{eff}^{m_{el}} \quad (6.11)$$

The constants  $C_{el}$  and  $m_{el}$  in Equation (6.11) can be calculated using Equations (6.12) and (6.13) and are functions of material parameters used in 'model F'. Equation (6.11) can be used to calculate crack propagation rates at small  $\Delta K_{eff}$ . A general crack propagation law, based on Equations (6.6) and (6.11) is presented in following Clause.

$$C_{el} = 2 \cdot \delta \cdot \left( (\sigma_f' - \sigma_m) \cdot \sqrt{2 \cdot \pi} \cdot \delta \right)^{\frac{1}{b'}} \quad (6.12)$$

$$m_{el} = -\frac{1}{b'} \quad (6.13)$$



**Figure 6.2 :** Substitutions made in order to obtain Equation (6.11).

Equation (6.12) contains the term  $\sigma_m$ , which can be used to take into account the effect of the local mean stress on the fatigue threshold. The  $\sigma_m$  can be expressed as a function of the effective stress intensity factor range  $\Delta K_{eff}$ , and the maximum effective stress intensity factor  $K_{max,eff}$  :

$$\sigma_m = C_m \cdot \left[ K_{eff,max}^{m_m} - \left( \frac{\Delta K_{eff}}{2} \right)^{m_m} \right] \quad (6.14)$$

Constants  $C_m$  and  $m_m$  in Equation (6.14) can be calculated using Equations (6.15) and (6.16) correspondingly. Derivation of Equations (6.14), (6.15) and (6.16) is explained in Annex A.4.2.

$$C_m = K' \cdot \left( \frac{n'+1}{\pi \cdot \delta \cdot E \cdot K'} \right)^{\frac{n'}{n'+1}} \quad (6.15)$$

$$m_m = \frac{2 \cdot n'}{n'+1} \quad (6.16)$$

### 6.1.3 Crack Propagation Rate Equation

The objective of this section is to propose a crack propagation rate equation. Further, the background of this equation is explained and the equation itself analyzed. The effective stress intensity factor range at the *intersection point* of the two curves given by Equations (6.6) and (6.11),  $\Delta K_{eff}^*$ , can be calculated using Equation (6.17) :

$$\Delta K_{eff}^* = \left( \frac{C_{el}}{C_{pl}} \right)^{\frac{1}{m_{pl}-m_{el}}} \quad (6.17)$$

The  $\Delta K_{eff}^*$  is a partition point of two regions of  $\Delta K_{eff}$ : *fatigue threshold* region with  $\Delta K_{eff} < \Delta K_{eff}^*$ , and *stable growth* region with  $\Delta K_{eff} > \Delta K_{eff}^*$ . Crack propagation rates  $da/dN$  within the fatigue threshold region can be calculated using Equation (6.11). Values for  $da/dN$  can be calculated within the stable growth region using Equation (6.6). Together, these equations lead to the general crack propagation rate equation (6.18), which can be used to calculate  $da/dN$  for any value of  $\Delta K_{eff}$ . The  $C_{el}$ ,  $m_{el}$ ,  $C_{pl}$  and  $m_{pl}$  in Equation (6.18) can be calculated using Equations (6.12), (6.13), (6.7) and (6.8), correspondingly.

$$\frac{da}{dN} = \frac{I}{\frac{I}{C_{el} \cdot \Delta K_{eff}^{m_{el}}} + \frac{I}{C_{pl} \cdot \Delta K_{eff}^{m_{pl}}}} \quad (6.18)$$

Three  $da/dN$ - $\Delta K_{eff}$  curves given by Equations (6.6), (6.11) and (6.18), are shown in Figure 6.3. It can be seen that Equation (6.18) ensures a smooth transition from the fatigue threshold region given by Equation (6.6), to the stable growth region given by Equation (6.11). The proposed law has a bi-slope form if plotted on log-log scale. Measured  $da/dN$  curves, if plotted versus  $\Delta K$ , also have two slopes: Herzberg [6.3], for example, shows the bi-slope  $da/dN$ - $\Delta K$  curves of 7075-T6. The same can be said about the  $da/dN$ - $\Delta K$  curves in [6.4], [6.5], [6.6].

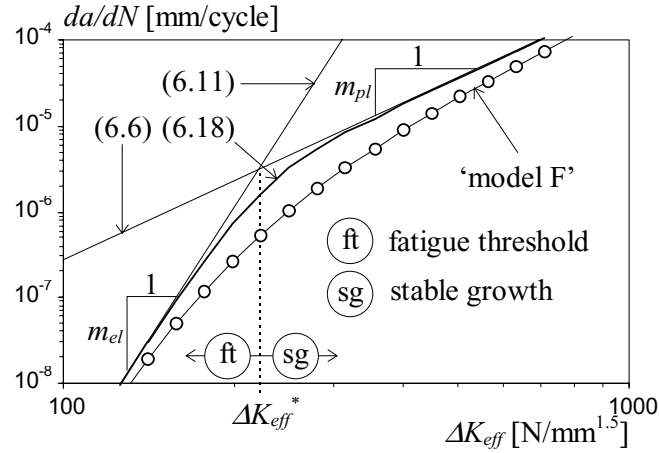


Figure 6.3 : Crack propagation rate curves for St50 [6.7].

The crack propagation rates, calculated using 'model F', are also given in Figure 6.3. It can be seen that Equation (6.18) leads to more conservative  $da/dN$ - $\Delta K_{eff}$  curves than 'model F'. The conservatism of Equation (6.18) arises due to the following reasons: Equation (6.11) was developed using only the *elastic* term, and Equation (6.6) using only the *plastic* term of the strain-life relationship and of the Ramberg-Osgood equation. In calculations of the  $da/dN$ - $\Delta K_{eff}$  curve by 'model F', both the elastic *and* plastic terms of the strain-life relationship and Ramberg-Osgood equation, are used. It is impossible to get an *analytical* formula for the  $da/dN$ - $\Delta K_{eff}$  curve using both elastic *and* plastic terms of the strain-life relationship and the Ramberg-Osgood equation. In 'model F', the calculation of the  $da/dN$ - $\Delta K_{eff}$  curve is made by *iteration*.

Equation (6.18) leads to a *non-fixed* fatigue threshold concept: if  $\Delta K_{eff}$  decreases then the corresponding crack propagation rates calculated using Equation (6.18) decrease exponentially

and crack propagation practically stops. On the contrary to the modified Paris law (2.27), Equation (6.18) does not require a special parameter to take account for the effect of the fatigue threshold.

The term  $C_{el}$  in Equation (6.18) is function of the local mean stress  $\sigma_m$ . The  $\sigma_m$  can be calculated using Equation (6.14) and is a function of the maximum effective stress intensity factor  $K_{eff,max}$ . An increase of  $K_{eff,max}$  results in an increase of  $C_{el}$  and a corresponding decrease of the fatigue threshold, which agrees with the test observations [6.3], [6.8].

Parameters  $C_{el}$ ,  $m_{el}$ ,  $C_{pl}$  and  $m_{pl}$  in Equation (6.18) can be calculated as functions of the constants of the strain-life relationship and Ramberg-Osgood equation. These constants are published for a great number of ductile materials [6.7]. Thus it is possible to rapidly compare the fatigue properties of different materials. An example of this is given in Figure 6.4. The comparison shows that StE790 steel has better fatigue properties than the St50 steel (i.e., both the fatigue threshold and the stable growth region of the StE790 are below the corresponding regions of the St50 steel.) Figure 6.4 also demonstrates that the proposed crack propagation equation can account for the influence of the nominal stress ratio  $R$ . It is well known that increasing  $R$  leads to decrease in fatigue threshold, which is well represented by curves in Figure 6.4. Published data also show that an increase in yield stress leads to increase in the fatigue threshold [6.9]. The comparison of StE790 and St50 steels shows the same tendency : the steel with a greater yield stress (StE790) has a greater fatigue threshold than the steel with lower yield stress (St50).

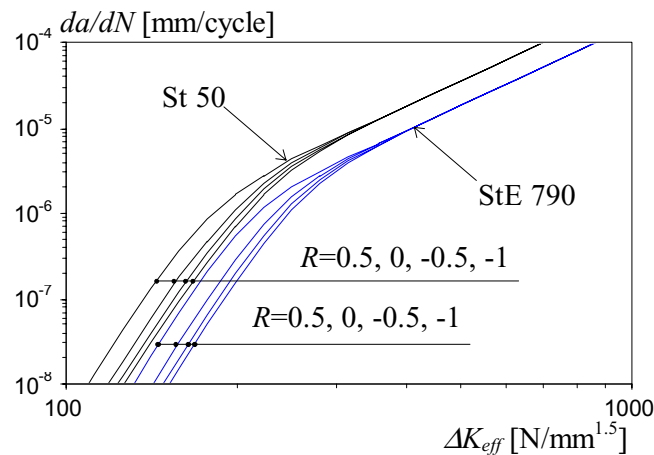


**Figure 6.4 :** A comparison in between the crack propagation rate curves of two materials.

Therefore, the proposed crack rate propagation equation (6.18) is developed on the basis of the modeling approach, presented in Chapter 3. There are some differences between Equation (6.18) and the conventional Paris law. Specifically, Equation (6.18) leads to the non-fixed fatigue threshold concept, it allows to account for the effect of maximum stress intensity factor  $K_{eff,max}$ , and the constants of this equation can be determined analytically. Equation (6.18) has a wide range of application possibilities. Some of these possibilities are reviewed later.

The summary of Section 6.1 is presented in Figure 6.5. On the basis of the *plastic* portion (2.19) of strain-life relationship, Equation (6.6) was developed in Clause 6.1.1. Equation (6.6) is similar to the Paris equation (2.25), and Equations (6.12) and (6.13) can be used to calculate the constants of the classical Paris equation. On the basis of *elastic* part (2.19) of strain-life relationship, Equation (6.11) was developed in Clause 6.1.2 in order to take into account the fatigue threshold. Finally, based on Equations (6.6) and (6.11), the crack propagation rate equation (6.18) was proposed in Clause 6.1.3.

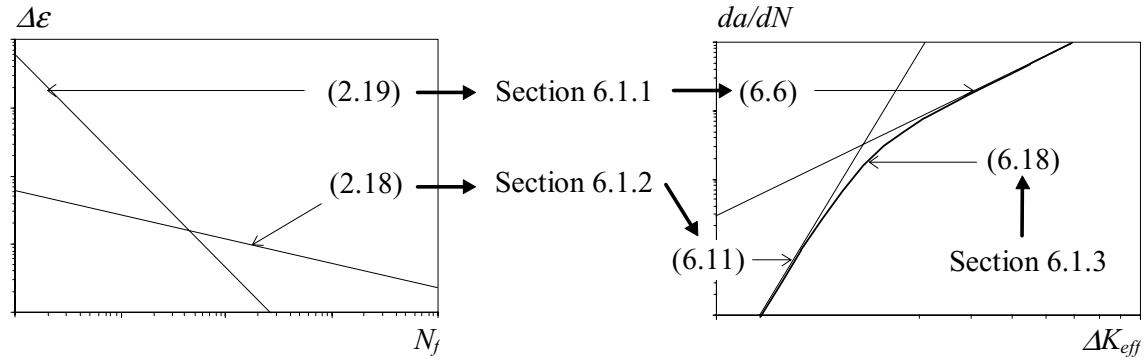


Figure 6.5 : Summary of Section 6.1.

## 6.2 SIMPLIFIED 'MODEL F' - 'MODEL SF'

The aim of this section is to introduce a simplified version of 'model F'. This simplified version is called 'model SF', where 'SF' stands for 'Simplified Fatigue'. The main requirement of the simplified fatigue crack propagation model is that it should be easily programmable for a personal computer yet remain general and precise enough for use in fatigue analysis. 'model SF' is based on the crack propagation rate Equation (6.18).

### 6.2.1 Calculation of Fatigue Life

#### Crack Initiation

The objective of this section is to demonstrate how Equation (6.18) can be used to evaluate the duration of the crack initiation stage,  $N_{CI}$ . Further, something uncommon will be done - a crack initiation period  $N_{CI}$  will be calculated on the basis of stress intensity factor. The only reason for this is to keep the calculation procedure simple. (i.e., to use similar formulas for both : crack initiation stage and the stable crack growth stage.)

In order to use Equation (6.18), the effective stress intensity factor range  $\Delta K_{eff}$  must be known. Since there is no fatigue crack present in the detail during the crack initiation stage,  $\Delta K_{eff}=0$  if it is calculated conventionally. In order to obtain an effective stress intensity factor range greater than zero, the  $\Delta K_{eff}$  is replaced by a *fictitious* stress intensity factor range  $\Delta K_{fict}$ . The fictitious stress intensity factor range is chosen so that it results in the same linear-elastic loading of the element  $k=j=1$  that is calculated using Equation (3.15). This condition can be expressed by Equation (6.19), where the right side of Equation (6.19) equals the right side of Equation (3.15), and its left side equals the right side of Equation (3.18) :

$$\Delta K_{fict} \cdot \sqrt{\frac{2}{\pi \cdot \delta}} = \frac{\Delta \sigma_0}{\delta} \int_0^{\delta} SCF(x) dx \quad (6.19)$$

Solving Equation (6.19) for  $\Delta K_{fict}$  gives :

$$\Delta K_{fict} = SCF^* \cdot \Delta \sigma_0 \cdot \sqrt{\pi \cdot \frac{\delta}{2}} \quad (6.20)$$

where  $SCF^*$  in Equation (6.20) stands for an average stress concentration factor over the length  $\delta$  of the element  $k=j=1$ . Very often the notation  $K_t$  is used instead of  $SCF^*$  in the literature. Herein  $SCF^*$  is used because 'K' already stands for the stress intensity factor and the monotonic strain hardening coefficient. Introducing  $\Delta K_{fict}$  into Equation (6.18) and

integrating Equation (6.18) over the first element at the crack initiator leads to the expression for the crack initiation life  $N_{CI}$  :

$$N_{CI} = \int_0^{\delta} \left( \frac{1}{C_{el} \cdot \Delta K_{fict}^{m_{el}}} + \frac{1}{C_{pl} \cdot \Delta K_{fict}^{m_{pl}}} \right) da = \frac{\delta}{C_{el} \cdot \Delta K_{fict}^{m_{el}}} + \frac{\delta}{C_{pl} \cdot \Delta K_{fict}^{m_{pl}}} \quad (6.21)$$

$\delta$  in Equation (6.21) can be seen as the initial crack length  $a_0$  and it can be taken :

$$a_0 = \delta = 0.1 \text{ [mm]} \quad (6.22)$$

$C_{el}$ , in Equation (6.21) can be calculated using Equation (6.12). The local mean stress,  $\sigma_m$  in Equation (6.12), can be calculated using Equation (6.14), where  $K_{eff,max}$  and  $\Delta K_{eff}$  in Equation (6.14) must be replaced by  $K_{max,fict}$  and  $\Delta K_{eff}$ , correspondingly. The fictitious maximum stress intensity factor  $K_{max,fict}$  can be calculated using Equation (6.23) which is similar to Equation (6.20).

$$K_{max,fict} = SCF^* \cdot \sigma_{0,max} \cdot \sqrt{\pi \cdot \frac{\delta}{2}} \quad (6.23)$$

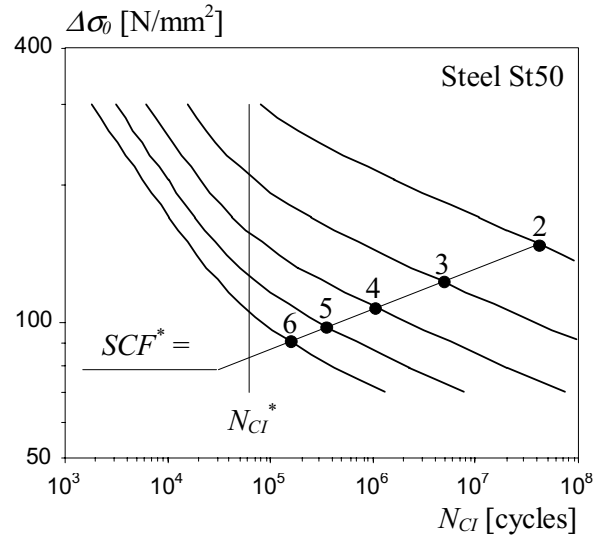


**Figure 6.6 :** The influence of an average stress concentration factor  $SCF^*$  on the  $N_{CI}$ .

Figure 6.6 presents an example of a crack initiation period, calculated as a function of an average stress concentration factor  $SCF^*$ . The material parameters of St50 steel were chosen to calculate the parameters of Equation (6.21). The local mean stress is taken as  $\sigma_m=0$ . It can be seen that the mean stress concentration factor has a very large influence on the crack initiation period  $N_{CI}$ . Figure 6.6 clearly illustrates that because the  $SCF^*$  of the welded details is very high, these details demonstrate a fast crack initiation period. The  $N_{CI}$  also depends on the nominal stress range  $\Delta\sigma_0$ . If  $\Delta\sigma_0$  is small, the crack initiation period increases significantly, regardless if the  $SCF^*$  remains high or not. Curves in Figure 6.6 have two slopes. This is because Equation (6.21) is a function of two terms. The knee-points  $N_{CI}^*$  of the  $\Delta\sigma_0$ - $N_{CI}$  curves can be calculated using Equation (6.24)

$$N_{CI}^* = \frac{\delta}{C_{el} \cdot \left(\frac{C_{el}}{C_{pl}}\right)^{\frac{m_{el}}{m_{pl}-m_{el}}}} = \frac{\delta}{C_{pl} \cdot \left(\frac{C_{el}}{C_{pl}}\right)^{\frac{m_{pl}}{m_{pl}-m_{el}}}} \quad (6.24)$$

It can be concluded that the use of the fictitious stress intensity factor range  $\Delta K_{fict}$  makes it possible to calculate the crack initiation period using  $da/dN$ - $\Delta K_{eff}$  curves.

### Total Fatigue Life

The total fatigue life  $N_f$  can be calculated using Equation (6.25). Parameters  $C_{el}$ ,  $m_{el}$ ,  $C_{pl}$  and  $m_{pl}$  in Equation (6.25) can be calculated using Equations (6.12), (6.13), (6.7) and (6.8), respectively. Equation (6.25) does not take into account the influence of simultaneous damaging. How to appropriately account for the effect of simultaneous damaging will be discussed in Clause 6.2.4.

$$N_f = N_{CI} + \int_{a_0}^{a_{cr}} \left( \frac{1}{C_{el} \cdot \Delta K_{eff}(a)^{m_{el}}} + \frac{1}{C_{pl} \cdot \Delta K_{eff}(a)^{m_{pl}}} \right) da \quad (6.25)$$

Integration of the total fatigue life using Equation (6.25) can result in very long computing time, especially if *small* nominal loads and/or *complex* loading histories are present. The increase in computing time is directly related to the fact that the effective stress intensity factor range  $\Delta K_{eff}$ , must be re-calculated every time the crack length  $a$  changes. The algorithm of the simplified model presented in Clause 6.2.4 will include some techniques to save computing time.

## 6.2.2 Effective Stress Intensity Factor Range

A parametric study carried out in Chapter 5 showed that the nominal load range is one of the most important fatigue parameters. In addition, the influence of the nominal mean load was shown to be important as well. According to the crack closure concept, only the effective part of the nominal load range causes the growth of the fatigue crack. If the reduction of the nominal load range due to the crack closure effect is not taken into account, the results of the fatigue analysis will be conservative.

The crack closure effect can be taken into account using the *effective* stress intensity factor range  $\Delta K_{eff}$  instead of the stress intensity factor range  $\Delta K$ . The  $\Delta K_{eff}$  is introduced because it is used in the crack propagation law (6.18). The objective of this section is to present a *simplified* method for calculating the  $\Delta K_{eff}$  due to both *constant-amplitude* and *variable-amplitude* loading.

### Constant-Amplitude Loading

The  $\Delta K_{eff}$  as a function of constant-amplitude loading can be calculated as follows :

- Using Equation (3.45) to find the nominal crack opening stress at a crack length  $a$ ,  $\sigma_{op}(a)$ .
- Calculate the crack opening stress intensity factor  $K_{op}$  using Equation (2.7) and substituting  $\sigma_{op}$  for  $\sigma_0$  in Equation (2.7).
- Using Equation (2.7), calculate the stress intensity factors due to the maximum and minimum nominal loads,  $K_{max}$  and  $K_{min}$ . Using Equation (2.8), calculate the stress intensity factor due to fabrication-introduced residual stress,  $K_{res}$ .
- Using Equations (6.26), (6.27) and (6.28), calculate the effective stress intensity factor range  $\Delta K_{eff}$ .

$$\Delta K_{eff} = K_{max} - K_{min} \quad \text{if} \quad K_{max} > K_{min} > (K_{op} - K_{res}) \quad (6.26)$$

$$\Delta K_{eff} = K_{max} - K_{op} \quad \text{if} \quad K_{max} > (K_{op} - K_{res}) > K_{min} \quad (6.27)$$

$$\Delta K_{eff} = 0 \quad \text{if} \quad (K_{op} - K_{res}) > K_{max} > K_{min} \quad (6.28)$$

### Variable-Amplitude Loading

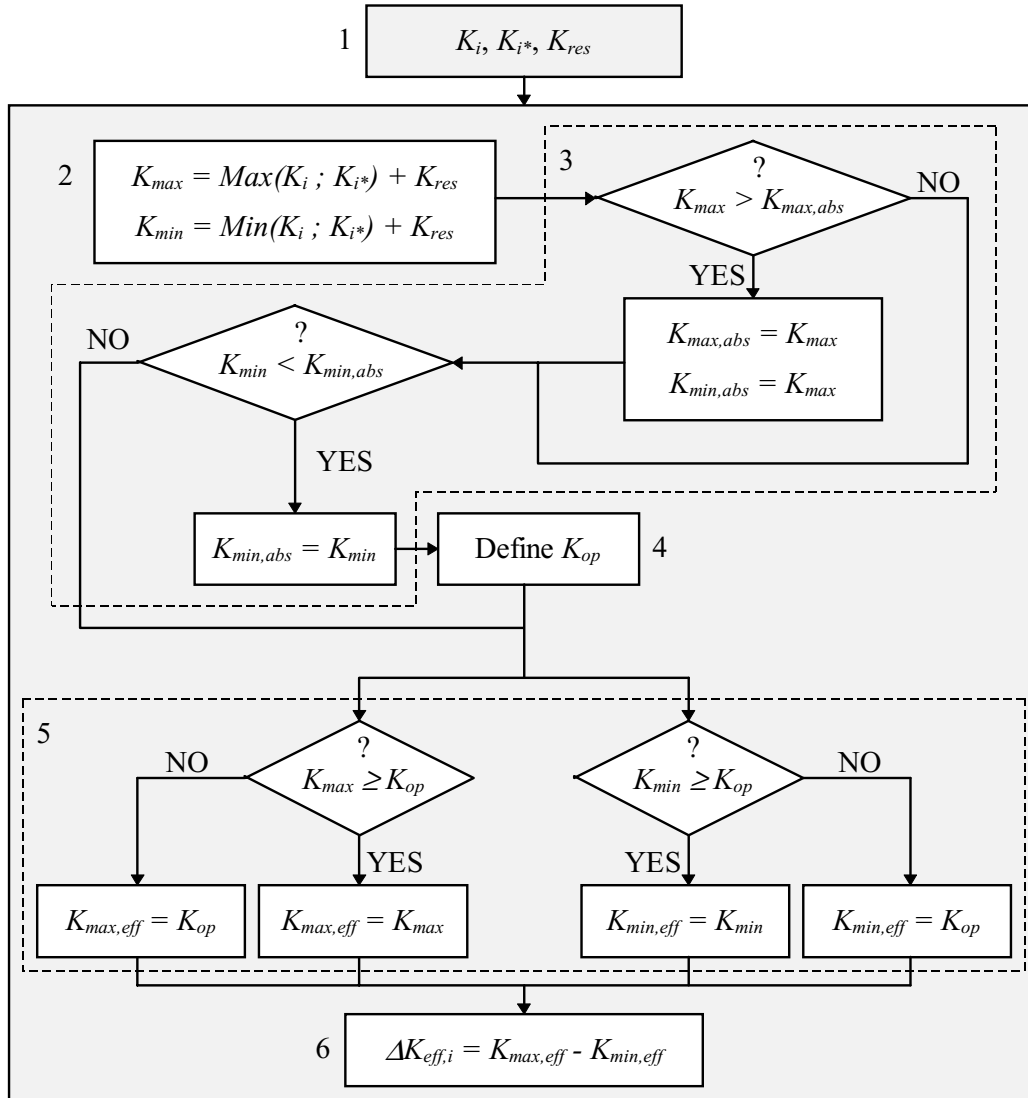


**Figure 6.7 :** Calculation algorithm of the effective stress intensity factor range.

The calculation algorithm for the effective stress intensity factor range  $\Delta K_{eff,i}$  corresponding to variable-amplitude load reversal, is presented in Figure 6.7. The following steps are needed :

1. Calculation of the stress intensity factors  $K_i$ ,  $K_{i^*}$  and  $K_{res}$ , as a function of the  $\sigma_{0,i}$ ,  $\sigma_{0,i^*}$  and fabrication induced residual stresses  $\sigma_{res}$ . The index\* in  $K_{i^*}$  corresponds to the nominal load peak that forms a closed stress-strain hysteresis loop with the load peak (see Clause 3.4.2). The  $K_i$  and  $K_{i^*}$  can be calculated using Equation (2.7), the  $K_{res}$  using Equation (2.8).
2. Determination of the  $K_{max}$  and  $K_{min}$  as functions of  $K_i$ ,  $K_{i^*}$  and  $K_{res}$ .
3. Re-compute, if necessary, the absolute maximum and minimum stress intensity factors  $K_{max,abs}$  and  $K_{min,abs}$ .
4. Calculation of the opening stress intensity factor  $K_{op}$  using Equation (6.29). The stress intensity factor  $K_{op}^*$  in Equation (6.29) corresponds to the stabilized crack opening stress  $\sigma_{op}$ , and can be calculated using Equation (3.47). Similar to Equation (3.45), Equation (6.29) takes into account the change in crack opening stress due to the change in

crack length, where  $K_{max,abs}(a-\delta)$  is the absolute maximum stress intensity factor just before the previous element breaks.

$$K_{op}(a) = K_{min,abs} + \frac{K_{max,abs}(a-\delta)}{K_{max,abs}} \cdot (K_{op}^* - K_{min,abs}) \quad (6.29)$$

5. Calculation of the effective stress intensity factors  $K_{max,eff}$  and  $K_{min,eff}$ .
6. Calculation of the effective stress intensity factor range  $\Delta K_{eff,i}$ .

Advantages of the proposed calculation method with respect to the effective stress intensity factor range are :

- It's *generality* : this method can be used to calculate the effective stress intensity factor ranges, within a large region, while still accounting for the influence of plate thickness, load history and yield stress, on the crack closure phenomenon. In addition, Equation (6.29) automatically takes into account increases in the crack opening stress intensity factor if the crack length increases.
- It's *simplicity* : the proposed formula are simple and the algorithm in Figure 6.7 is linear. No iterations are needed in order to calculate  $\Delta K_{eff,i}$ .
- It's *rapidity* : the proposed method leads to a very fast calculation of the effective stress intensity factor ranges. A big advantage, when compared to existing crack closure approaches, can be obtained. This is especially true when the influence of a *complex* load history is analyzed.

### 6.2.3 Algorithm

The aim of this section is to present the overall algorithm of the simplified fatigue crack propagation model - 'model SF'. The algorithm of 'model SF' is shown in Figure 6.8 and the steps in computing it are reviewed later.

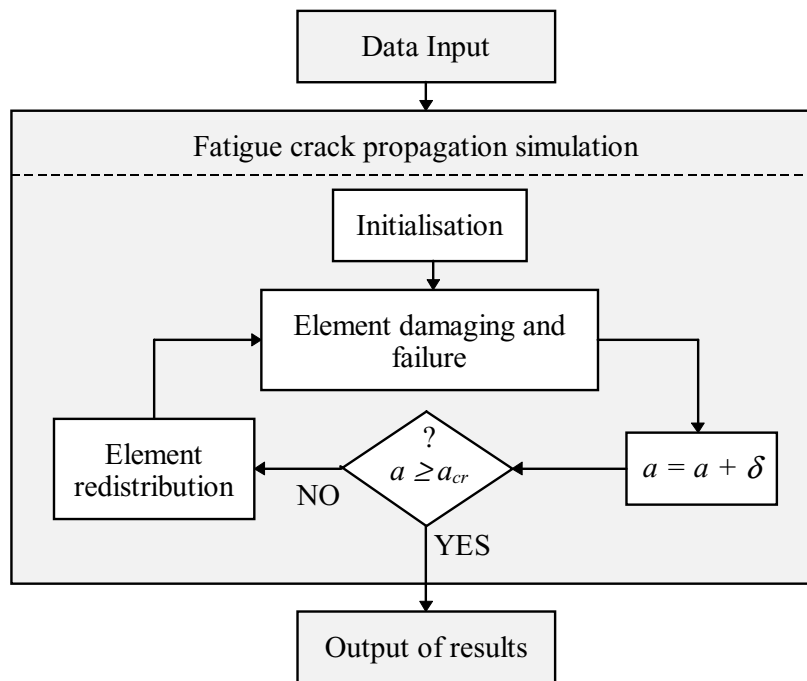


**Figure 6.8 :** The overall algorithm of 'model SF'.

### Data Input

Similar to 'model F', there are three groups of input data required : *loading history*, *detail geometry* and *material properties*. The input data should be made as described in Clause 3.6.1.

### Initialization

Initialization of the 'model SF' includes the following tasks :

- *Rainflow analysis* of the load history in order to determine the tips of the stress-strain hysteresis loops (see Clause 3.4.2).
- *Set up of elements*. The elements are placed close to the stress concentrators and amount of elements used at the same time in the calculations should not exceed 5.
- Determination of *average stress concentration factors*  $SCF_k^*$ , for elements  $k=1...5$ . The  $SCF^*$  is required for the crack initiation stage only.
- Determination of the *stress intensity correction factor*  $Y_k$ , for elements  $k=(1), 2...n_{global}$ . ( $Y_1=0$  if no initial crack is assumed to be in the detail).
- Calculation of the material-related parameters  $m_{el}$ ,  $C_{pl}$  and  $m_{pl}$  used in the crack propagation rate law (6.18). Parameter  $C_{el}$  in Equation (6.18) is a function of  $\Delta K_{eff}$  and  $K_{eff,max}$  and therefore can not be pre-computed.
- Calculation of constants  $\phi_{el}$  and  $\phi_{pl}$ . These constants are used in order to take account for the simultaneous damaging of the elements. Calculation of the  $\phi_{el}$  and  $\phi_{pl}$  differs whether in the crack initiation stage or in the stable crack growth stage :
  - *crack initiation stage* :

$$\phi_{el,k} = \left( \frac{SCF_k^*}{SCF_1^*} \right)^{m_{el}} \quad (6.30)$$

$$\phi_{pl,k} = \left( \frac{SCF_k^*}{SCF_1^*} \right)^{m_{pl}} \quad (6.31)$$

- *stable crack growth stage* :

$$\phi_{el,j} = \left( \sqrt{j} - \sqrt{j-1} \right)^{m_{el}} \quad (6.32)$$

$$\phi_{pl,j} = \left( \sqrt{j} - \sqrt{j-1} \right)^{m_{pl}} \quad (6.33)$$

where  $k=1...5$  in Equations (6.30) and (6.31), and  $j=1...5$  in Equations (6.32) and (6.33).

### Element Damaging and Failure

The algorithm for element failure and simultaneous damaging is given in Figure 6.9 and includes the following steps :

- *Initialization* of the damage calculation loop which contains the initialization of the reversal counter ( $n=0$ ) and determination of the crack propagation stage. It is assumed that the *crack initiation* stage changes into the *stable crack growth* stage when the element at the crack initiator ( $k=1$ ) is broken.
- Calculation of the *effective stress intensity factor range*  $\Delta K_{eff,i}$ . Calculation of the  $\Delta K_{eff,i}$  depends on the crack propagation stage : if crack initiation takes place,  $\Delta K_{eff,i}$  must be calculated using Equation (6.20) at the stable crack growth stage using the algorithm presented on Figure 6.7.

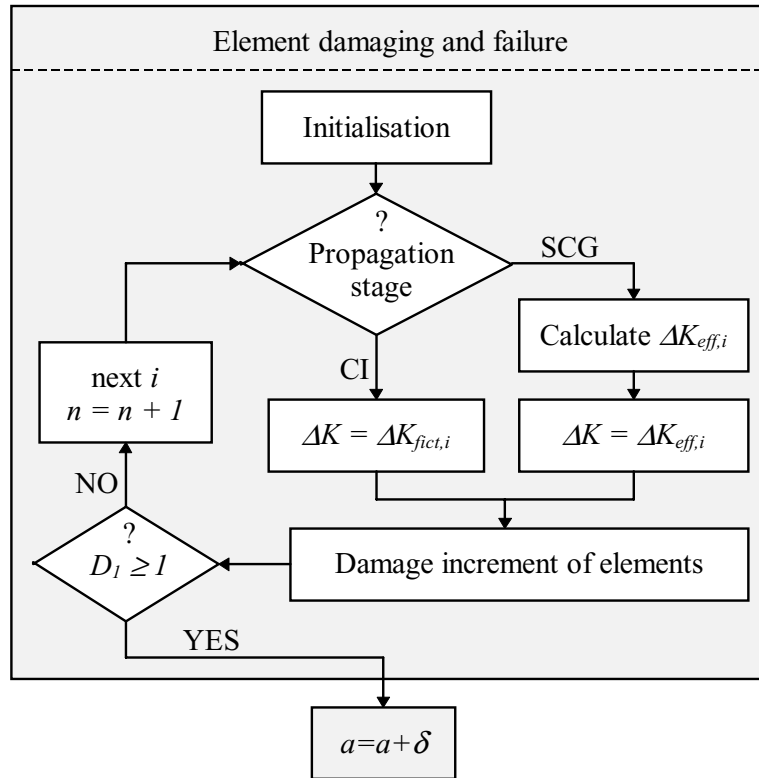


Figure 6.9 : Algorithm of the element failure and simultaneous damaging.

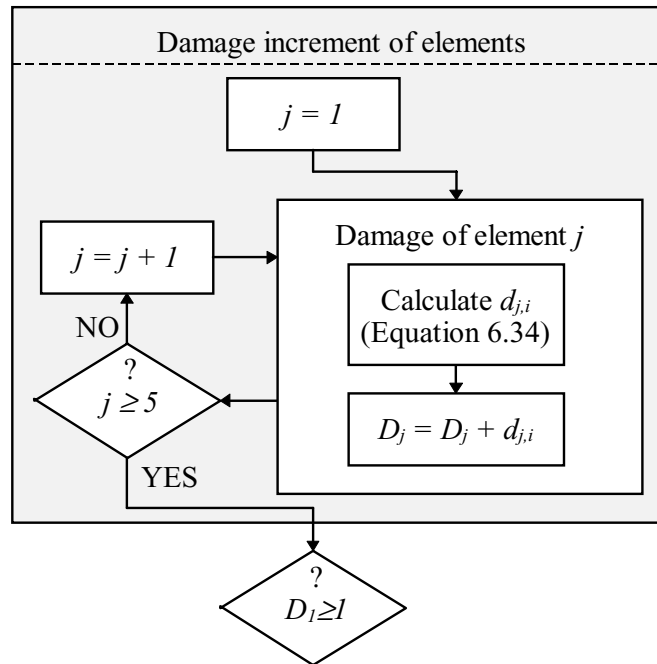


Figure 6.10 : Algorithm of the damage increment of elements.

- *Damage increment of elements.* This calculation step is presented in Figure 6.10 and it consists of looping, where within every loop, the damage increment of the element  $j$ ,  $d_{j,i}$  is

calculated<sup>1</sup>. This can be made using Equation (6.34). Then the  $d_{j,i}$  is added to the total damage of the element  $j$ ,  $D_j$ . Looping is continued until the damage increment of all 5 elements is found.

$$d_{j,i} = \frac{1}{2 \cdot \delta} \cdot \left( \frac{1}{\frac{1}{\phi_{el,j} \cdot C_{el} \cdot \Delta K_{eff,i}^{m_{el}}} + \frac{1}{\phi_{pl,j} \cdot C_{pl} \cdot \Delta K_{eff,i}^{m_{pl}}}} \right) \quad (6.34)$$

- Check if the element  $j=1$  has failed. If the damage of element  $j=1$  is greater or equal to 1, then it is assumed that the first element has failed. Otherwise the damage increment of the elements is calculated using the next load reversal,  $i$ .

### **Increment of the Crack Length**

After failure of the element  $j=1$ , the crack length  $a$  is increased by the element size  $\delta$ . Then, the new crack length  $a$  is compared to the critical crack length  $a_{cr}$ . If  $a \geq a_{cr}$ , then the calculation is finished, and the output is written, else the elements are redistributed.

### **Redistribution of Elements**

Since the element  $j=1$  has failed, it is removed and a new element is added. The redistribution procedure is similar to the procedure described in Clause 3.6.2 : the intermediate results are saved, the elements re-numerated and the new element is added at the crack propagation path. The initial damage of the new element,  $D_5$ , can be calculated using Equation (3.39). Finally, the absolute maximum and the absolute minimum stress intensity factors  $K_{max,abs}$  and  $K_{min,abs}$ , must be re-calculated as indicated in Clause 3.5.3.

### **Output of Results**

In this step all the results are written in a result file. This can be made as described in Clause 3.6.3.

## **6.2.4 Verification of 'model SF'**

In chapter 4 'model F' was compared to fatigue test results. In this clause, the same is done using 'model SF'. In addition to comparing it to the test results, 'model SF' is compare to 'model F'.

### **Comparison to Test Results**

As an example, one series of comparisons is shown. Fatigue test for these comparisons are taken from Section 4.2.1 corresponding to the plate with a welded attachment. It should be noted that welded details have relatively short crack initiation lives compared to their total fatigue life. The needle peened specimen under constant-amplitude and spectrum A and B loading is used for verification of 'model F'. Specimen geometry and loading conditions are given in Figure 4.2 and Figure 4.3, respectively.

Comparisons between 'model SF'-simulated results and data from section 4.2.1 are presented in Figure 6.11. Each comparison includes two types of curves :  $a-N$  curves and  $da/dN-a$  curves. The variation of the simulated curves is obtained by changing the weld toe angle  $\alpha$  and the distribution of the residual stress (see Figure 4.2).

<sup>1</sup> Factor 2 in denominator of Equation (6.34) counts for the damage due to load reversal  $i$ . If damage due to load cycle is calculated, then factor 1 must be used instead.

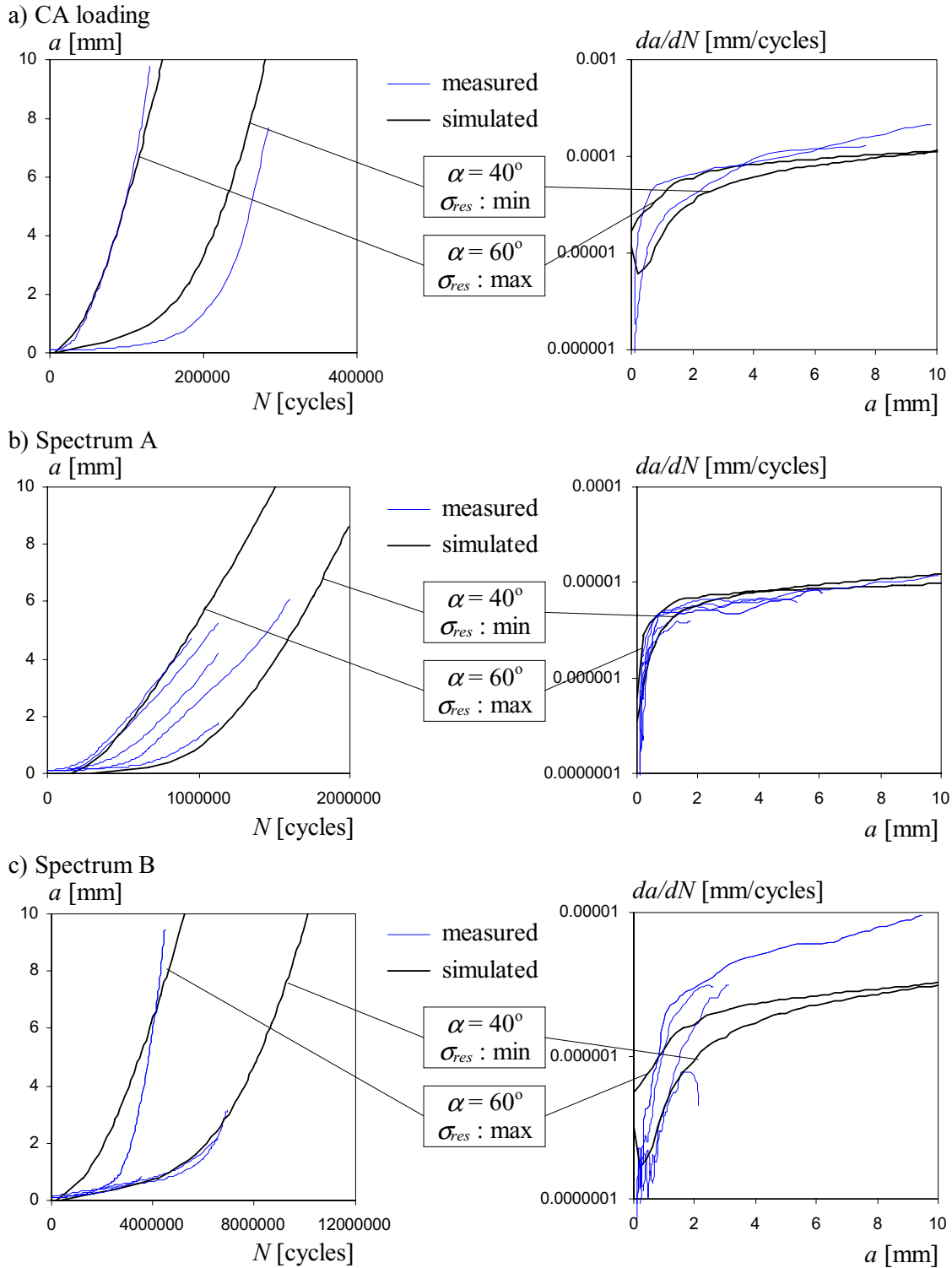


**Figure 6.11 :** Comparison of 'model SF' to the test data [4.1] : a) constant-amplitude loading ; b) spectrum A ; c) spectrum B.

Comparisons show that 'model SF' is able to simulate fatigue behavior of specimens of complicated geometry, taking into account the influence of residual stresses and varying loading conditions. This conclusion is valid for welded details having relatively short crack initiation life compared to their total fatigue life.

### Comparison to 'model F'

The second series of comparisons are made between 'model SF' and 'model F'. Two types of crack propagation is simulated by the models; 1) retardation effect of the overload and; 2) influence of mean stress.

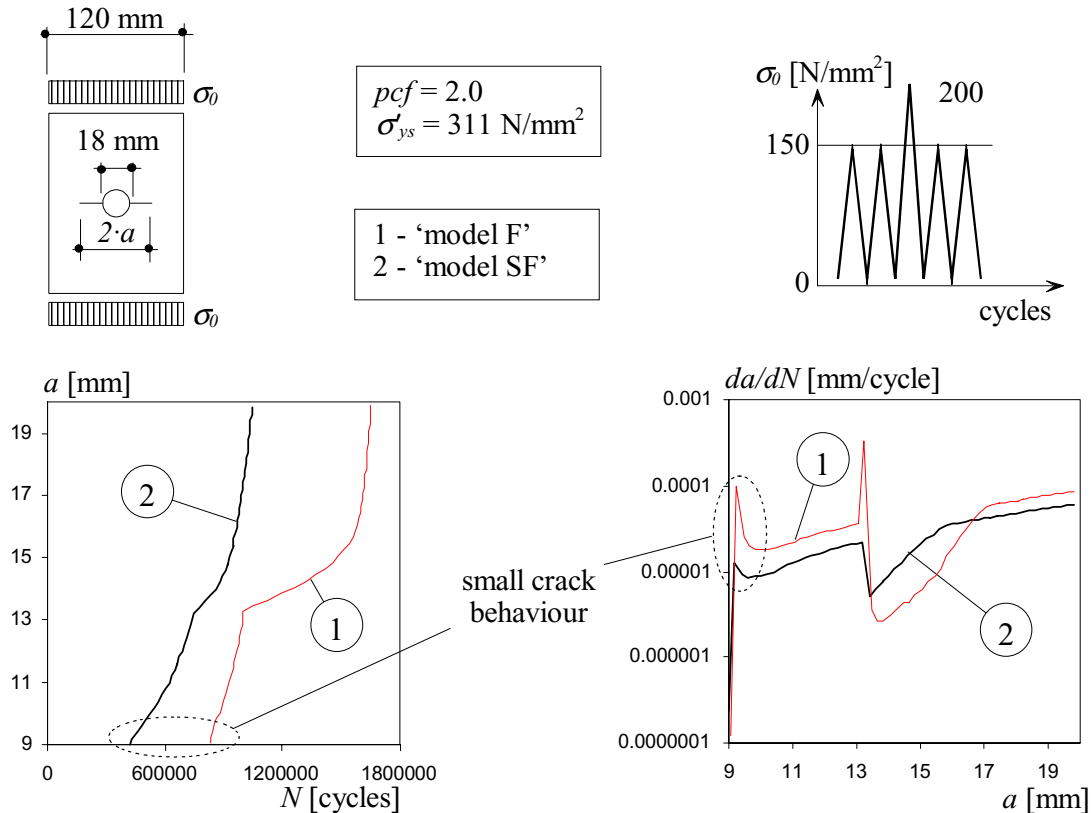


**Figure 6.12 :** Comparison between 'model SF' and 'model F' : retardation effect due to tensile overload.

Figure 6.12 presents the effect of tensile overload on fatigue behavior, simulated using 'model SF' and 'model F'. Figure 6.13 presents the influence of changing the nominal mean stress. The results are given as  $a$ - $N$  curves and  $da/dN$ - $a$  curves. These curves reveal the following :

- it appears that similar to 'model F', 'model SF' can simulate small crack behavior, but crack propagation rates of small cracks predicted by 'model SF' are smaller than those predicted by 'model F'.
- The crack initiation life simulated by 'model SF' is much shorter than the crack initiation life predicted by 'model F'. This is because 'model SF' is based on the crack propagation rate equation (6.18) which *always* leads to greater crack propagation rates than the strain life relationship (3.11) which used as the basis of 'model F' (see also Figure 6.3).
- The stable crack growth life predicted by 'model SF' is longer than that predicted by 'model F'. This is because the *effective* stress intensity ranges calculated by 'model F' are smaller than those found by 'model SF'. Correspondingly, 'model SF' predicts shorter retardation of crack propagation due to tensile overload than 'model F' (Figure 6.12). In addition, the influence of the change in nominal mean stress on crack propagation is also less important if calculated using 'model SF' rather than using 'model F' (Figure 6.13).

- It appears that ‘model SF’ is not able to consider a short acceleration in crack propagation just after application of the tensile overload. Since this acceleration is very short, it is not important to take it into account.

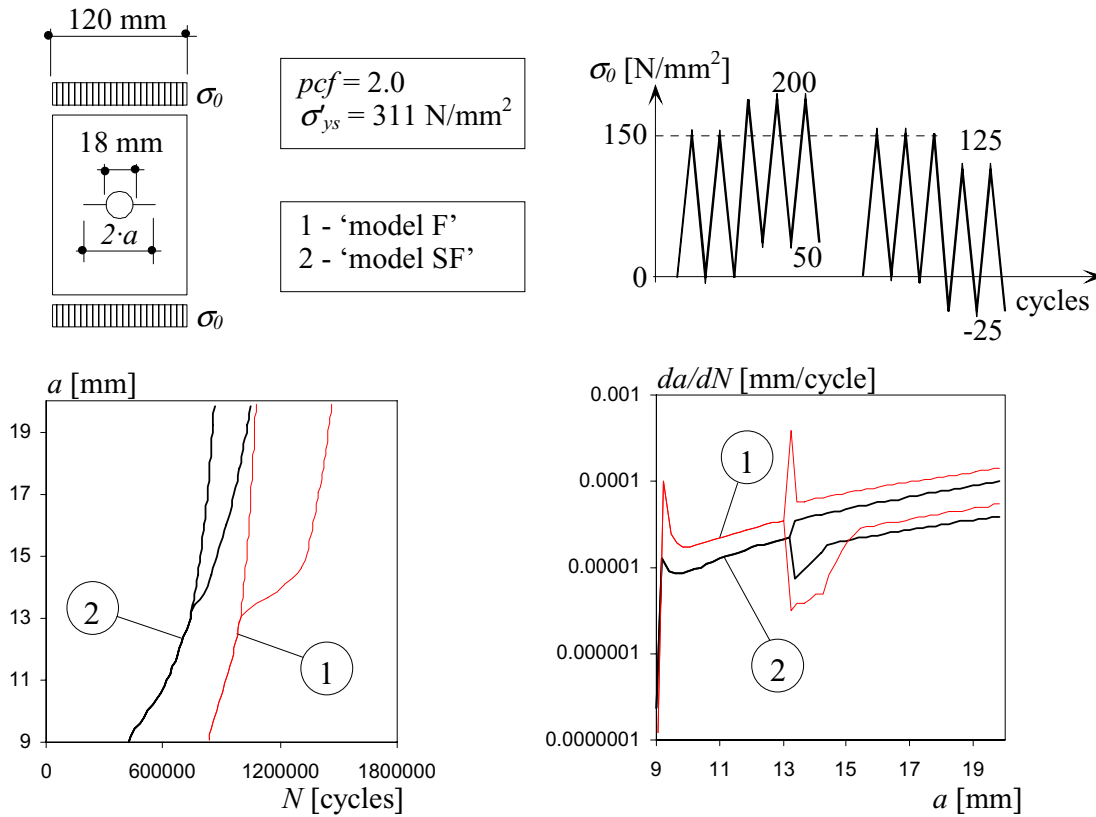


**Figure 6.13 :** Comparison of ‘model SF’ to ‘model F’ :change in mean stress and small crack behavior.

It can be concluded that ‘model SF’ and ‘model F’ result in approximately the same results in cases when the crack initiation life is small compared to total fatigue life. On the other hand, in cases where crack initiation life constitutes a large portion of the total fatigue life, ‘model F’ leads to shorter crack propagation than ‘model SF’.

## 6.2.5 Discussion of ‘model SF’

This section reviews the basic assumptions, outlines the advantages and disadvantages, and establishes the application limits and application field of simplified model - ‘model SF’.

### Assumptions

‘Model SF’ is based on a crack propagation rate equation (6.18) which was developed on the basis of strain-life relationships (2.18) and (2.19), Glinka’s ESED criterion and Ramberg-Osgood equations (3.19) and (3.20). The above mentioned equations and relationships are related to each other according to the principles used in ‘model F’. These principles are reviewed and analyzed in Chapter 3, including use of the  $SCF(x)$  and  $Y(a)$  in order to characterize the linear-elastic stress field at a stress concentrator using the average value of the same linear-elastic stress as element loading, etc.. The basic assumptions considering ‘model SF’, are :

- Elements represent the average material fatigue behavior along their length. Elements are placed along crack propagation path, where the latter is situated perpendicular to the maximum principal tensile stresses occurring in the specimen due to nominal loading.
- Fatigue life of elements can be calculated using strain-life relationships obtained by smooth specimen fatigue testing (see Clause 3.3.2). For that, it is assumed that if elements, placed on the surface of smooth specimen, at a crack initiator or, at a fatigue crack tip, are loaded by equal strain ranges, then the fatigue lives of these elements are equal.
- The crack initiation stage finishes after the element at the crack initiator fails. This assumption was largely confirmed by fatigue analysis carried out using 'model F'.

### ***Advantages and Disadvantages***

The *advantages* of the 'model SF' are :

- The constants of the crack propagation rate law can be evaluated using material data obtained from smooth specimen testing. A large range of these data are available in the literature. In addition, the proposed crack propagation rate equation does not require any special considerations to take into account the fatigue threshold.
- The crack initiation period can be evaluated, using the same approach and the same material constants used to calculate the duration of the stable crack growth period.
- A simplified crack closure model accounts for the increase in fatigue life due to the crack closure effect. In addition, the evolution of the opening stress intensity factor, as function of crack length, is considered.
- 'Model SF' accounts for the influence of fabrication-introduced residual stresses and the effect of the simultaneous damaging. This gives the model the ability to simulate small crack behavior, without adding any special features.

The *disadvantages* of 'model F' are :

- Greater initial efforts are needed to put the proposed approach into computer code than if the conventional fracture mechanics approach was used. However, the increase in the range of application is many times greater than the loss in time invested in programming.
- Since the fatigue analysis is carried out using *average* material data, safety factors should then be applied to the results if used for fatigue design. The calculation of the appropriate safety factors is out of the scope of this study.

### ***Application Field and Application Limits***

Based on the modeling assumptions, as well as on the comparisons of 'model SF' to test data and to 'model F', it can be said that 'model SF' can be used in fatigue analysis for specimens of any geometry and containing any distribution of residual stress. Covered materials include structural steels of ductile stress-strain behavior. Since features to consider crack closure effect are included, 'model SF' is able to account for the influence of variable-amplitude loading on fatigue behavior.

However, the maximum applied loads should not cause large scale yielding of the net section. This condition must be guaranteed in order to ensure that small scale yielding conditions are present at the crack tip (see condition (5.20)). The limits on element size  $\delta$  are established by condition (5.19). If 'model SF' is applied on the analysis of details made of aluminum, the limits of the element size should be reviewed. This is due to fact that micro-structure of aluminum differs from that of steel.

Finally, it must be said that like 'model F', 'model SF' is a deterministic model and therefore does not take into account variation of material properties. Due to its wide application range and relative simplicity, 'model SF' can, however, be supplemented by including statistical aspects of the material properties into the model.

## 6.3 APPLICATION EXAMPLES

The objective of this section is to present two examples of how ‘model SF’ and ‘model F’ can be applied to fatigue analysis. The examples include :

- The study of fatigue properties of structural steels by means of crack propagation rate equation (6.18).
- Comparison of variable-amplitude fatigue analysis carried out by ‘model F’ to similar analysis made using  $S-N$  curves and linear damage accumulation rule.

### 6.3.1 Analysis of Material Parameters

In this section, two topics are presented : the comparison of fatigue properties of structural steels with the aid of the crack propagation equation (6.18), leading to recommendations concerning the choice of the material.

#### *Influence of Steel Grade*

Comparison is made between five structural steels : St37, St42, St46, St50 and St52. The material properties needed to calculate the constants  $C_{el}$ ,  $m_{el}$ ,  $C_{pl}$  and  $m_{pl}$  used in Equation (6.18), are taken from [6.7]. The local mean stress  $\sigma_m$  in Equation (6.12) is taken 0. Figure 6.14 represents 25  $da/dN-\Delta K_{eff}$  curves calculated using 25 sets of the material data from [6.7]. The raw material of the test specimens were treated by high temperature in some cases.

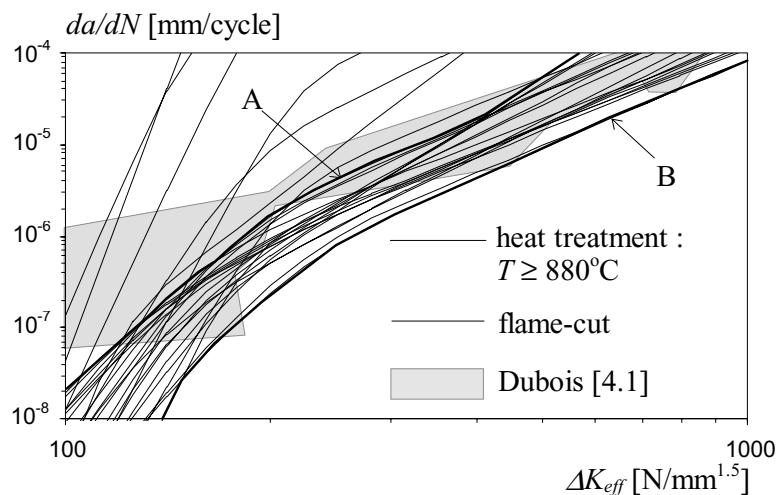


**Figure 6.14 :** Crack propagation rate curves for unalloyed steels St37, St42, St46, St50 and St52.

A comparison of the curves show that :

- the  $da/dN-\Delta K_{eff}$  curves of the steels analyzed generally fall within a relatively narrow scatter band. The boundaries of the scatter in crack propagation rate curves are marked with A and B in Figure 6.14. A scatter band of crack propagation rate curves measured by Dubois [4.1], are shown in same figure. It appears that  $da/dN-\Delta K_{eff}$  curves predicted using Equation (6.18) correspond quite well with results of Dubois [4.1]. Differences between measured and predicted curves are observed in the region of small  $\Delta K_{eff}$ . This can be explained by the fact that in the analysis of test results, Dubois did not take into account the

effect of small crack behavior and therefore obtained relatively high crack propagation rates at small values of  $\Delta K_{eff}$ .

- The effective threshold stress intensity factor range  $\Delta K_{eff,th}$  at the crack propagation rate  $da/dN_{th}=10^{-8}$  mm/cycle is :

$$\Delta K_{eff,th} = 100...130 \text{ [N/mm}^{1.5}] \quad (6.35)$$

- An analysis shows the large influence of heat treatment on crack propagation rate - heating the material to a temperature of  $T > 880^\circ\text{C}$  leads to catastrophic loss in fatigue properties. The curves of heat-treated materials (dotted curves in Figure 6.14), are out of the region that is bounded with curves A and B. Figure 6.14 also shows the negative influences of flame cutting on fatigue properties<sup>1</sup>.
- If heat treatment is made under a temperature of  $T < 660^\circ\text{C}$ , then the curves of fatigue crack propagation rate fall within the region that is bounded by curves A and B.

Comparison showed that high temperature has a very large influence on the fatigue properties of material. This implies that the material inside the heat affected zones around welds can lose a considerable part of its fatigue resistance.

Constants  $C_{el}$ ,  $m_{el}$ ,  $C_{pl}$  and  $m_{pl}$  used in Equation (6.18) are sensitive to the constants of the strain-life relationship. The constants of the strain-life relationship can be determined by fatigue testing of a smooth specimen, but a large amount of these constants are available in the literature [6.7].

Even though fatigue properties of structural steels are within a relatively narrow scatter band, the fatigue life of two identical details made of different steel can, however, differ many times. Fatigue design with the steel with 'good' fatigue properties allows a remarkable gain in fatigue life.

### Choice of Material for Fatigue Design

Based on Figure 2.17 and on the modeling principles, the following recommendations can be made, in order to select the material :

- If the detail contains *high* local stress concentrations (*welded* details, for example) then a *ductile* material should be chosen. The use of a ductile material leads to a slower stable crack growth compared to tough or strong materials, the crack initiation stage of this type of details is short regardless the type of material.
- If the detail contains *small* or *medium* local stress concentrations (details with holes and smooth notches, for example) then a *strong* material should be chosen. The use of a strong material leads to a longer crack initiation stage compared to tough or ductile materials, the stable crack growth stage of this type of detail is short compared to the crack initiation, regardless the type of material.
- If the detail is made of a *composite material*, then for the first layer, a *strong* material should be used which leads to a long crack initiation life. Other layers should be made of a *ductile* material that makes the stable crack growth stages slower than if tough or strong materials were used.

### 6.3.2 'model F' versus S-N Curves

Even though *S-N* curves are normally used for fatigue *design* and not for prediction of fatigue *life*, sometimes they are used in order to evaluate (remaining) fatigue life of existing structures. It is interesting to show the difference in prediction of the fatigue life made using 'model F' and *S-N* curve. The aim of this section is to *compare* the fatigue lives  $N_f(MF)$  obtained using 'model F', to the fatigue lives  $N_f(SN)$  obtained by means of the *S-N* curve.

<sup>1</sup> The dotted curve noted 'flame-cut' in Figure 6.14 corresponds to the point 'flame-cut' in Figure 5.13.

The fatigue life  $N_f(MF)$  is obtained by numerical simulations using ‘model F’. The *detail geometry* used in simulations is a plate with hole. The dimensions of the plate are identical to those used in the parametric study (Figure 5.1). The *material properties* used are given in Table 5.2. Simulations with ‘model F’ were carried out under variable-amplitude loading. The 64 *load histories* used were calculated in the way shown in Annex A.4.3. The fatigue life  $N_f(MF)$  is calculated in units of *load history*.

The fatigue life  $N_f(SN)$  is calculated as follows :

- firstly, the rainflow analysis of the 64 load histories (see Annex A.4.3), identical to those used in numerical simulations, is carried out in order to obtain the load spectra.
- Secondly, using Equation (6.36), the damage due to every load spectrum, is calculated. Since the plate with hole corresponds to the detail category 90 in [6.10], the double-slope fatigue resistance curve of the *DC90* (Figure 5.18) is used to calculate  $N_{f,i}$  in Equation (6.36).

$$d_{ls} = \sum_i \frac{n_i}{N_{f,i}} \quad (6.36)$$

Depending on the load range level  $\Delta\sigma$  in spectrum, the  $N_{f,i}$  in Equation (6.36) is calculated using Equations (6.37), (6.38) or (6.39) :

$$\Delta\sigma_i \geq \Delta\sigma_D : \quad N_{f,i} = \frac{\Delta\sigma_D^{m_1} \cdot N_D}{\Delta\sigma_i^{m_1}} \quad (6.37)$$

$$\Delta\sigma_{CUT-OFF} \leq \Delta\sigma_i < \Delta\sigma_D : \quad N_{f,i} = \frac{\Delta\sigma_D^{m_2} \cdot N_D}{\Delta\sigma_i^{m_2}} \quad (6.38)$$

$$\Delta\sigma_i < \Delta\sigma_{CUT-OFF} : \quad N_{f,i} \rightarrow \infty \quad (6.39)$$

where the constants in Equations (6.37), (6.38) and (6.39) correspond to the fatigue resistance curve *DC90*, and they are :

$$\begin{aligned} \Delta\sigma_D &= 66 \text{ [N/mm}^2\text{]} \\ m_1 &= 3 \\ N_D &= 5 \cdot 10^6 \text{ [cycles]} \\ \Delta\sigma_{CUT-OFF} &= 36 \text{ [N/mm}^2\text{]} \\ m_2 &= 5 \end{aligned}$$

- The fatigue life  $N_f(SN)$ , is calculated in units of *load spectra* using Equation (6.40), where the damage due to one load spectrum  $d_{ls}$  in Equation (6.40) is calculated using Equation (6.36).

$$N_f(SN) = \frac{1}{d_{ls}} \text{ [load spectra]} \quad (6.40)$$

In comparisons, all variable-amplitude load histories are normalized using the equivalent constant-amplitude stress range  $\Delta\sigma_e$ , which can be calculated using Equation (5.17). The results of comparison are presented in Figure 6.15. The comparison shows that if  $\Delta\sigma_e > 100 \text{ N/mm}^2$ , use of *S-N* curve leads approximately the same fatigue life as ‘model F’. On the other hand, the difference between fatigue lives predicted using ‘model F’ and *S-N* curves increases if  $\Delta\sigma_e$  decreases. Within the range  $36 \leq \Delta\sigma_e \leq 80 \text{ N/mm}^2$ , this difference is at least *three* times. If the equivalent constant-amplitude stress range is less than the cut-off limit, then both ‘model F’ and *S-N* curves predict fatigue threshold.

There are two reasons why the *S-N* curves lead to more conservative results than does ‘model F’ for use in prediction of fatigue life for details loaded by variable-amplitude loading.

First, use of the *linear* damage accumulation rule instead of non-linear rule leads to shorter fatigue lives. Second, *S-N* curves correspond to fatigue lives *reduced* by a safety factor. In the example given, fatigue lives predicted by *S-N* curves are not much shorter than those calculated using 'model F'. This is because the mean stress in the load histories used for the simulations are high. The 'conservatism' of the *S-N* curves would be larger if load histories with lower mean stresses (with compressive nominal stresses), were used. It should be noted that the comparison made is valid, however, for the given detail geometry and material properties only.

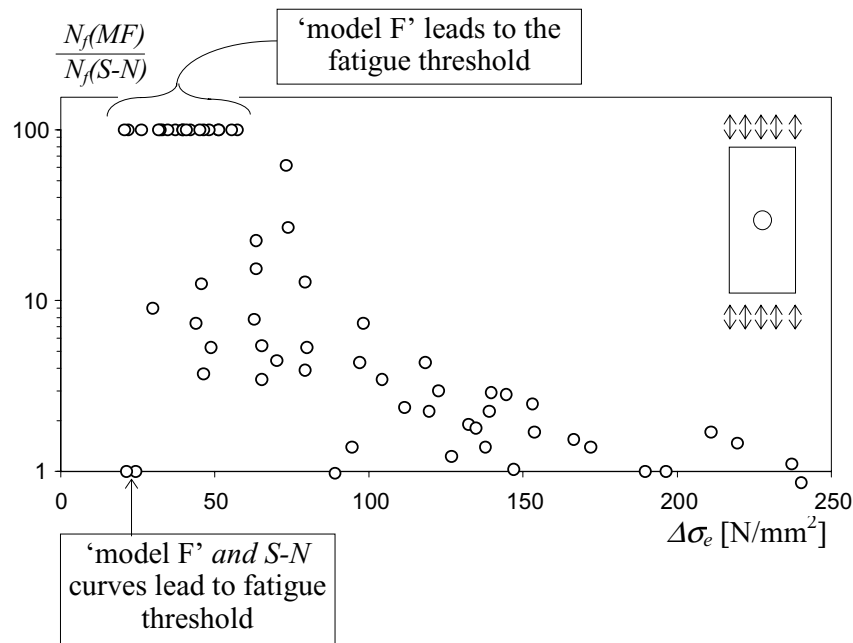


**Figure 6.15 :** The comparison of variable-amplitude fatigue analysis made using 'model F' and *S-N* curves.

## 6.4 SUMMARY

### 'Model F' versus Paris Equation

In the first part of Chapter 6, a crack propagation rate equation was developed. This equation leads to results similar to the Paris equation. There are three advantages of the proposed equation compared to Paris equation. First, the constants of Equation (6.18) can be determined without testing (i.e., they can be calculated using the material constants of the strain-life relationship and Ramberg-Osgood equation). Second, Equation (6.18) accounts for the fatigue threshold without introducing an extra parameter into crack propagation rate equation. Third, the proposed equation accounts for the effect of the maximum stress intensity factor on the crack propagation rate.

### 'Model SF'

Computational procedures used in 'model F' are relatively complex : they include a number of iterations and rather involved algorithms. A simplified crack propagation model - 'model SF' was developed on the basis of 'model F'. It leads to similar results as a fatigue analysis conducted using 'model F', but uses much simpler computing procedures and algorithms.

'model SF' is based on the crack propagation rate equation (6.18). It allows calculation of the fatigue life by taking into account all important aspects of fatigue crack propagation: the influence of the crack initiation and stable crack growth stages, the crack closure effect, the small crack behavior, the effect of residual stresses, etc. An original crack closure model, presented in Chapter 3, is simplified and introduced into 'model SF'. Working algorithms of 'model SF' are also given. 'Model SF' is compared to fatigue test data and to 'model F', its advantages and disadvantages outlined, and application limits and application field established.

### ***Application Examples***

Two examples were introduced in order to show how the approaches developed can be used in fatigue analysis. The first example showed how the crack propagation rate equation (6.18) can be used to compare the fatigue properties of steels. Comparison of structural steels St37, St42, St 46, St50 and St 52 showed that their fatigue properties are relatively similar and that heat treatments at high temperatures ( $T > 880^{\circ}\text{C}$ ) significantly reduce the fatigue resistance of these materials. The recommendations concerning the choice of the material were also given.

In the second example, fatigue lives obtained using 'model F' were compared to fatigue lives obtained using the  $S-N$  curves. The comparison showed that use of the  $S-N$  curve for variable-amplitude fatigue analysis of a plate with center hole predicts shorter fatigue lives than 'model F', especially in the region of a small equivalent constant-amplitude stress range.